HHS Public Access

Author manuscript

IEEE Trans Ultrason Ferroelectr Freq Control. Author manuscript; available in PMC 2020 July 20.

Published in final edited form as:

IEEE Trans Ultrason Ferroelectr Freq Control. 2016 May ; 63(5): 671–682. doi:10.1109/TUFFC.2016.2531504.

Targeted Lesion Generation Through the Skull Without Aberration Correction Using Histotripsy

J. R. Sukovich,
Department of Biomedical Engineering, University of Michigan, Ann Arbor, MI 48109 USA

Z. Xu,
Department of Biomedical Engineering, University of Michigan, Ann Arbor, MI 48109 USA and also with the Department of Pediatrics, University of Michigan, Ann Arbor, MI 48109 USA

Y. Kim,
Department of Biomedical Engineering, University of Michigan, Ann Arbor, MI 48109 USA

H. Cao,
Department of Biomedical Engineering, University of Michigan, Ann Arbor, MI 48109 USA

T.-S. Nguyen,
Department of Biomedical Engineering, University of Michigan, Ann Arbor, MI 48109 USA

A. S. Pandey,
Department of Neurosurgery, University of Michigan, Ann Arbor, MI 48109 USA

T. L. Hall,
Department of Biomedical Engineering, University of Michigan, Ann Arbor, MI 48109 USA

C. A. Cain
Department of Biomedical Engineering, University of Michigan, Ann Arbor, MI 48109 USA

Abstract

This study demonstrates the ability of histotripsy to generate targeted lesions through the skullcap without using aberration correction. Histotripsy therapy was delivered using a 500 kHz, 256-element hemispherical transducer with an aperture diameter of 30 cm and a focal distance of 15 cm fabricated in our lab. This transducer is theoretically capable of producing peak rarefactional pressures, based on linear estimation, $(p\text{-})_{LE}$, in the free field in excess of 200 MPa with pulse durations ≤2 acoustic cycles. Three excised human skullcaps were used displaying attenuations of 73–81% of the acoustic pressure without aberration correction. Through all three skullcaps, compact lesions with radii less than 1 mm were generated in red blood cell (RBC) agarose tissue phantoms without aberration correction, using estimated $(p\text{-})_{LE}$ of 28–39 MPa, a pulse repetition frequency of 1 Hz, and a total number of 300 pulses. Lesion generation was consistently observed at the geometric focus of the transducer as the position of the skullcap with respect to the transducer was varied, and multiple patterned lesions were generated transcranially by mechanically adjusting the position of the skullcap with respect to the transducer to target different regions within. These results show that compact, targeted lesions with sharp boundaries can be

Corresponding: Jonathan R. Sukovich jsukes@umich.edu.

generated through intact skullcaps using histotripsy with very short pulses without using aberration correction. Such capability has the potential to greatly simplify transcranial ultrasound therapy for non-invasive transcranial applications, as current ultrasound transcranial therapy techniques all require sophisticated aberration correction.

Keywords

Transcranial therapy; histotripsy; non-invasive therapeutic ultrasound; cavitation; aberration correction

I. Introduction

The effects of high intensity focused ultrasound (HIFU) on human and animal brains have been studied extensively to show the feasibility of using ultrasound therapies in the brain with portions of the skullcap removed since the 1950's [1]–[4]. Non-invasive ultrasound therapies for the brain, however, have been limited due to the presence of the skullcap in the acoustic field. Since the 1970's [5], a number of techniques have been developed to enable ultrasound transcranial therapy. Recently, major efforts in this field have explored a variety of non-invasive therapy possibilities for diverse applications such as tumor ablation [6], treatment of brain disorders [7], [8], thrombolysis [9]–[11], and drug delivery [12], [13] with promising results. At the time of this writing, initial clinical trials on using magnetic resonance guided focused ultrasound (MRgFUS) for essential tremor and Parkinson's disease were underway with FDA approval in the United States [8], and the first MRgFUS brain tumor ablation case in human has been reported [14].

For transcranial ultrasound therapy, a skullcap in the ultrasound pathway causes significant attenuation and defocussing (aberration effects) to the ultrasound signals passing through it. The high attenuation and strong phase aberrations introduced by the skullcap [15] can significantly distort the shape of pressure field and decrease its amplitude at the treatment site, thereby limiting the treatment's effectiveness. Many sophisticated techniques have been studied to account for these aberrations by measuring the phase distortions introduced by the skull and by using phased array ultrasound sources to correct for them and improve the focal pressure profile at the treatment site [16]–[20]. For example, MRgFUS uses the skullcap profile extracted from prior 3D CT scans of the patient's brain to calculate and compensate for the aberrations introduced by the skullcap. However, during MRgFUS treatment, as it is impossible to put the patient in the exact same position as the previous scan, MRI is needed to guide and monitor precise energy deposition and focusing through the skullcap [16], [19], [20].

Acoustic time-reversal is another widely studied method to correct for aberrations [18], [21] that relies on using reference acoustic signals to adjust the firing phase of individual elements of a phased array transducer to compensate for temporal aberrations introduced to the ultrasound pulses by the skull. Acquiring the reference signals necessary for time-reversal non-invasively, however, requires a reference signal to be emitted from within the skullcap and a phased array transducer with sophisticated driving electronics capable of transmitting and receiving signals at each element of the array in order to record the signals

necessary for time-reversal. In a recent study examining the feasibility of accomplishing non-invasive time-reversal correction by using acoustic signals emitted by individual bubbles in the brain as the reference signals, individual bubbles were initially generated with only coarse aberration correction [18].

Additionally, because bone is a strong absorber of ultrasound [22]–[24], temperatures at the skullcap surface must be monitored during HIFU treatments to prevent overheating and thermal damage to the skull bone and the brain tissue adjacent to it. Current HIFU systems address this issue by actively cooling the scalp using a continuously circulating refrigerated water bath as the coupling medium for the ultrasound [21], [25]. Even with active cooling, however, it may still be necessary to limit the ultrasound power applied during HIFU treatments to prevent thermal damage [20]. Cavitation therapy has been studied as an alternative ultrasound treatment for transcranial applications [11], [26], [27] and may help to reduce the overheating associated with typical HIFU therapies [16] owing to the shorter duty cycle pulses required to generate cavitation bubble clouds. In these types of therapies, cavitation bubble clouds are generated using high intensity pulsed ultrasound applied at low duty cycles to ablate tissues in their vicinity while minimizing thermal exposure.

A method that can generate precise lesions transcranially without aberration correction while minimizing heating to the skullcap would be a very useful advancement for non-invasive transcranial therapy. A number of studies have shown that lower amplitude ultrasound pulses in combination with ultrasound contrast agents can be used to generate cavitation through the skull to open and facilitate drug delivery through the blood brain barrier [28]–[31] and to enhance clot thrombolysis during stroke [32]–[35] in a targeted fashion. However, precise lesion generation through an intact skullcap, without any external agents or complex aberration correction schemes, remains technically challenging because it requires both sufficiently high pressures and a highly focused ultrasound beam to be maintained through the highly attenuative and aberrative skull.

Histotripsy is an ultrasound therapy that uses high-pressure, short duration pulses to generate targeted energetic cavitation bubble clouds to mechanically fractionate tissue. Histotripsy can generate a cavitation bubble cloud using a single short ($\leq$2 acoustic cycles), high-amplitude ultrasound pulse where the peak negative pressure exceeds the intrinsic threshold for nucleation of the media (26–30 MPa peak rarefactional pressure, $(p\text{-})_{LE}$, in high water content tissues) [36]. This makes histotripsy particularly robust even in situations where severe aberrations are introduced to the ultrasound pulses [37], as damage generated by histotripsy is well confined to only the regions where the pressure exceeds the intrinsic threshold for nucleation, and as the short duration ultrasound pulses used for therapy minimize the side lobes of the focal region and thereby limit cavitation nucleation events outside of the target area. In addition, because damage is confined only to the regions where the pressure exceeds the intrinsic threshold for cavitation, histotripsy may be used to generate sub-wavelength sized lesions, corresponding to the size of the region within the negative acoustic half-cycle where the pressure exceeds the intrinsic threshold for nucleation of the media [38], [39]. As only a single pulse of less than 4 microseconds is necessary to generate the cavitation, and an arbitrarily low duty cycle can be used for therapy (e.g., $<$0.01%), thermal effects can also be minimized during histotripsy treatments.

In a recent study by Kim *et al.* [40], the feasibility of using histotripsy to generate lesions transcranially was explored. A 500 kHz 32-element hemispherical transducer with an aperture diameter of 30 cm and a focal distance of 15 cm was used to deliver histotripsy therapy to a red blood cell (RBC) tissue phantom through an intact human skullcap. Phase adjustment was applied to the ultrasound pulses in that study to achieve $(p\text{-})_{LE}$ in the focal zone of 29 to 30 MPa to exceed the intrinsic threshold necessary to generate cavitation. With only 32 elements and coarse aberration correction, histotripsy was demonstrated to be able to generate single lesions as small as 0.7×1.6 mm in the RBC phantoms.

In this paper we study histotripsy's ability to produce targeted lesions through the skullcap without using aberration correction. A new 500 kHz 256-element phased array was constructed to allow us to achieve p- exceeding the intrinsic threshold without using any correction at all. In the study by Kim *et al.*, only one skull sample was used, while in this study, we use three skulls with different characteristic dimensions and attenuations. We also investigate whether lesion generation at the focus of the transducer through the skullcap is appreciably affected by the position of the skullcap with respect to the transducer. Finally, we demonstrate that histotripsy can be used to generate arbitrarily shaped patterned lesions through the skullcap by mechanically moving the skullcap, and therefore the target region within, with respect to the transducer.

II. Materials and Methods

A. Phased Array Transducer

In these experiments histotripsy therapy was delivered using a 256-element hemispherical phased array transducer with an aperture diameter of 30 cm and a focal distance of 15 cm (Fig. 1). The transducer elements populating the array are 20 mm diameter flat, stacked piezo ceramic (PZ36) discs with center frequencies of 500 kHz. The transducer was constructed in our lab using the 3D rapid prototyping method as described in [41]. The elements were driven using a custom 256-channel high-voltage pulser developed in-house, capable of delivering short ($\leq$2 acoustic cycles) high amplitude ultrasound pulses to the transducer's focus during treatment (a characteristic focal pressure waveform measured in the free field may be seen in Figure 4(a)). The high-voltage pulser driving the transducer elements was controlled using a field-programmable gate array (FPGA) which allowed for the independent triggering of each channel of the array to deliver the ultrasound pulses. Individual elements were capable of generating peak rarefactional pressures at the transducer focus of 0.8 MPa at their maximum driving voltage, as measured with a high-sensitivity needle hydrophone (model HNR-0500, Onda Corp., Sunnyvale, CA) factory calibrated over a range of frequencies from 250 kHz-20 MHz, with a linear response up to approximately 2 MPa at 500 kHz. The pressure outputs of individual elements of the array were measured using the needle hydrophone before they were populated into the array. These measurements were taken individually with the needle hydrophone mounted coaxially with the array elements at a distance of 15 cm from the element's face, corresponding to the focal distance of the array. This theoretically allows for peak rarefactional pressures of the fully populated array, by linear summation of the contributions from individual elements, in excess of 200 MPa. This estimated $(p\text{-})_{LE}$ matched with the direct measurement from a fiber

optic hydrophone [42] up to 20 MPa. However, because cavitation exists 100% of the time above the intrinsic threshold, rarefactional pressures beyond 27–30 MPa are unlikely to be generated, much less measured, in high water content tissues. Due to this, precise pressure measurements of rarefactional pressures nearing or beyond the intrinsic threshold cannot be made and as such, stated rarefactional pressures beyond 20 MPa throughout the body of this paper are estimated by linear summation of the measured peak negative pressure amplitudes of individual transducer elements used to generate lesions during experiments. This method of estimating pressures has been shown to agree well with direct pressure measurements at pressures up to and beyond the intrinsic threshold in water [36]. While the accuracy of this method has been shown to have a dependence on the geometry of the transducer, and shown errors in the actual focal pressures of up to 15%, we used this method for predicting cavitation activity at the focus of the transducer used here as well as for estimating the available pressure overhead during treatments. As such it is not intended to serve as an actual measure of pressure, but rather an indication of the likelihood of cavitation activity in the focal region.

B. Sample Preparation

Transcranial experiments were conducted with 3 human cadaver skullcap samples obtained through the University of Michigan Anatomical Donations Program. The specimens were cleaned and defleshed after extraction and were continuously kept in water thereafter. Prior to experiments the skullcaps were degassed inside a vacuum chamber for one week. The physical dimensions of the skullcaps used in experiments were acquired from measurements made around the base of the skullcaps along the planes along which they were cut and may be seen in Table I.

The red blood cell (RBC) agarose tissue phantoms used in experiments consist of a thin layer (≤500 μm) of RBC's sandwiched between two layers of agarose gel. At 21 °C these blood cell phantoms were found to have a mean denisity of 1.02 ± 0.016 g/cm^3, a sound speed of 1501 ± 2 m/s, and an attenuation relative to water of 0.11 ± 0.017 dB/cm at 1 MHz. These RBC phantoms were prepared in square support frames, measuring $4 \times 4 \times 1.5$ cm, developed in house to allow ultrasound transmission towards the transducer focus. When exposed to cavitation, the cells in the RBC layer lyse and change from opaque to translucent, allowing for visual inspection of the damaged area during and after treatment. The cavitation threshold and lesions generated in the RBC phantoms have been shown to mirror very closely lesions produced in high water content tissues at equivalent exposure levels [36]. A complete description of these phantoms may be found in [43].

C. Full Field Hydrophone Measurements

Measurements of the pressure field were carried out using a fiber optic hydrophone built in house [42]. Measurements of the pressure field, in both the transcranial and free field cases, were carried out at a fixed rarefactional pressure amplitude at the focus of 18 MPa in order to ensure cavitation activity at the tip of the hydrophone during measurements was avoided, and to ensure measurements at comparable focal pressure amplitudes in the free field and transcranial cases were acquired. Measurements of the free field pressure field were acquired by scanning the fiber optic hydrophone across the geometric origin of the transducer, defined

as the center point of a spherical volume concentric with the hemishpherical array, in increments of 0.5 mm in straight lines measuring 2 cm in length, centered about the transducer's origin. At each measurement location, signals from 100 pulses of the transducer were acquired and averaged together to obtain the final pressure measurement. These measurements were repeated across the three ordinate directions of the transducer, corresponding to transverse/aperture (**x–y**) directions and axial (**z**) direction of the transducer, respectively.

For measurements of the pressure field in the transcranial cases, the skullcaps were mounted in the water tank in a fixed position with respect to the histotripsy transducer such that the focal point of the transducer lay within the caps of the skulls 5 mm beyond the plane along which the cap of the skull was cut (Fig. 2). The skullcaps were mounted centrally within the transducer such that the front and back, and left and right extremities of the skullcaps were equidistant from the interior surface of the transducer, respectively. During these measurements the hydrophone was initially placed at the location in the field where the negative pressure amplitude was found to be maximal, and measurements in the ordinate directions about this point were repeated as described above. Note of the initial location of the hydrophone with respect to the geometic origin of the transducer was made during the transcranial measurements in order to monitor for shifts in the transducer's focus in comparison to the free field case.

Measurements of the attenuations of the skullcaps were carried out using the fiber optic hydrophone. In these experiments the transducer was driven at a fixed power level such that in the free field case the pressure amplitude produced at the geometric origin of the transducer was measured to be 18 MPa. Driving the transducer at the same power level, measurements were repeated for the transcranial cases at the location in the field where the negative pressure amplitude was found to be maximal. The ratios of the transcranial and free field negative pressure amplitudes were taken and used to determine the attenuations of the skullcaps (calculated as $(1 - P_{tc}/P_{ff}) \times 100\%$, where P_{tc} and P_{ff} correspond to the transcranial and free field negative pressure amplitudes, respectively).

D. Cavitation and Lesion Imaging

Cavitation bubble clouds and resulting lesions were optically imaged using a high-speed, 1 megapixel CCD camera, (Phantom V210 - Vision Research, Wayne, New Jersey, USA). Images were captured in the transverse/aperture plane of the transducer and were backlit using laser light scattered off the interior surface of the skullcap (Figs. 1 & 3). The camera shutter speed was varied over a range of 10 to 40 μs between experiments to ensure sufficient backlighting for imaging. The camera was triggered in such a way that the cavitation bubble cloud and the lesion generated after each pulse were captured during histotripsy treatment.

For the single lesion generation experiments, the skullcaps were mounted in the water tank in the same fashion as described in Section II-C. The RBC phantoms were then positioned within the skullcap at the focus of the transducer for treatment and imaging.

During experiments studying patterned lesion generation and lesion generation as a function of skullcap position with respect to the transducer, the skullcap and RBC phantom were mounted in fixed positions with respect to one another via optical rods and attached as a single unit to a 3-axis positioner which allowed for the position of the assembly within the transducer, and thereby the target site of the histotripsy treatment, to be adjusted mechanically. This mounting setup ensured that we were able to capture images of lesions generated through the skullcap in the RBC phantom as the position of the skullcap/RBC phantom pair was moved with respect to the transducer. During these experiments, the initial position of the skullcap with respect to the transducer was set in the same way as described in the previous paragraph.

E. Histotripsy Treatment

The histotripsy treatments were delivered using high-amplitude, short duration (≤ 2 acoustic cycles) ultrasound pulses at pulse repetition frequencies (PRF) of 1 Hz. Lesions were generated in the RBC layers by applying a total of 300 histotripsy pulses at each treatment site. Images of the bubble clouds and the resultant lesions were captured after each histotripsy pulse during treatment and were imaged in the transverse plane of the transducer using the methods described in Section II-D.

For the single lesion generation experiments, RBC phantoms were treated through all three skullcap samples using histotripsy pulses with estimated negative pressure amplitudes at the focus of between 28 and 39 MPa. These pressure values were calculated by multiplying the measured attenuation values of the skullcaps by the free field $(p\text{-})_{LE}$ at an equivalent driving power of the array. This corresponds to a pressure well above the threshold for cavitation in sheep brain tissue of 22 MPa given in [26] as well as that for high water content tissues in general of 26–30 MPa given in [36]. In experiments studying patterned lesion generation and lesion generation as a function of skullcap position with respect to the transducer, only skullcap 3 was used. During these experiments, the skullcap/RBC phantom pair were moved in the transverse plane of the transducer as described in Section II-D in 4 mm increments to produce lesions in a 5×5 square grid measuring 1.6 cm per side. Lesions were generated in this experiment using histotripsy pulses with estimated peak negative pressure amplitudes at the focus of the transducer of 39 MPa.

III. Results

A. Hydrophone Measurements

Focal pressure measurements were collected to evaluate the amount of insertion loss introduced by the skullcap in comparison to free field conditions. The dimensions and thicknesses of the three skullcaps used during experiments are listed in Table I. The thicknesses of the skullcaps ranged from 2–12 mm as measured at different locations along the cut planes of the three samples. The presence of the skullcaps significantly attenuated the peak rarefactional pressure at the focus to approximately 19–27% of the value obtained in free field without using aberration correction.

Typical pressure waveforms measured at the focus of the transducer in the free field and through the three skullcaps without aberration correction are shown in Figure 4. It can be seen that the presence of the skullcaps in the sound field only minimally affects the shapes of the high amplitude portions of the pressure waveforms as they cross the transducer's focus in comparison to the free field, and that the waveforms are seen to maintain only a single high amplitude negative acoustic half-cycle responsible for generating cavitation. A small temporal advance of the peak negative pressure of between 1–2 μs is observed in the transcranial cases in comparison to the free field case, as was expected owing to the higher sound speed of bone than water. Based on measurements of the average thicknesses of the skullcaps and measured temporal advances, the calculated average sound speed for the three skullcaps was 2216±135 m/s, which lies within the bounds of previously reported values for the average sound speed of the skull in the frequency range between 0.3–0.8 MHz of 2291±160 m/s to 2408±112 m/s [44]. It can also be seen at later time points in Figures 4(b)–(d) that reverberations of the sound field within the skullcaps are apparent, however the pressure amplitude beyond the initial high amplitude portion of the pulse is significantly reduced and well below the threshold for nucleation.

Spatial profiles of the pressure fields through the three skullcap samples in the transverse (**x**) and axial (**z**) directions of the transducer are shown in Figure 5. There is good agreement between the free-field and transcranial pressure profiles through all three skullcap samples out to at least −5 dB, with slightly widened main lobes through the skullcaps as may be seen in Table II. Importantly, it can be seen that while the prefocal side lobes of the pressure field in the axial direction of the transducer are increased through the skullcaps, the position of the focal point itself is observed to shift only minimally as may be seen in comparison with the overlays of the free field pressure profiles in Figures 5(d)–(f), with a maximum observed focal shift of 550 μm in the post-focal direction. There is similarly good agreement between location of the focal points seen in the pressure profiles in the transcranial and free field cases in the transverse/aperture (**x**–**y**) direction of the transducer, with a maximum observed focal shift of 500 μm. Table II shows the −3 dB widths of the pressure profiles through all three skullcap samples in the transverse and axial directions of the transducer's focus. Compared to the −3 dB width of 1.09 × 1.12 × 2.35 mm in free field, the −3 dB width was increased the most by skullcap 3 to 1.96 × 1.26 × 2.64 mm. Through the skullcaps, side lobes of the pressure field in the axial direction were widened and had higher amplitude. The highest side lobes were seen at approximately −5 dB through the skullcaps, compared to −10 dB in the free field.

B. Transcranial Single Lesion Generation without Aberration Correction

In this study we were able to generate cavitation bubble clouds and lesions in the RBC phantoms at the transducer's focus through all three skullcap samples without using aberration correction. Typical images of the bubble clouds and the lesions generated through the different skullcap samples may be seen in Figure 6. Bubble clouds in each case were observed to form consistently after each histotripsy pulse applied during treatment. The bubble clouds generated through the skullcaps were typically compact and well confined to within the focal region, with only minor satellite, or incidental, bubble formation observed outside the region. Similarly, lesions generated through all three skull samples were typically

compact with only minor extraneous lesion formation observed outside of the main focal region as may be seen in Figs. 6(b) & 6(d), where small incidental lesions are observed to have formed a short distance away from the main central lesions.

For each skullcap sample, 7–11 lesions were generated in the RBC phantoms to obtain representative measurements of the cavitation clouds and lesions. Lesions were evaluated by binarizing the captured images and measuring the area of the contiguous fractionated regions at the end of each treatment to calculate lesion radii. Bubble cloud radii were calculated by constructing composite images of all the bubble clouds generated during each histotripsy treatment, and measuring the contiguous area over which bubbles were observed to have formed in the focal region. The measurements of the bubble clouds and lesions generated through the different skullcap samples may be seen in Table III. It can be seen that the lesions generated through all three skullcaps had similar radii on the order of between 600 and 660 μm, while the bubble clouds responsible for generating them were slightly larger, averaging between about 730 and 770 μm. The average extent of the lesions generated through the three skullcaps was observed to be on the order of between 70%−90% percent of the mean −3 dB width of the focal beam through the respective skullcaps, as measured in the transverse plane of the transducer (Table II).

C. Lesion Generation as a Function of Skullcap Position with Respect to the Transducer and Patterned Lesion Generation without Aberration Correction

To study the ability to generate lesions through the skullcap with the skullcap/RBC phantom pair at different positions with respect to the transducer without aberration correction, a 5 × 5 grid of lesions was formed through skullcap 3 by mechanically moving the skullcap/RBC phantom pair in 4 mm increments over a square region measuring 1.6 × 1.6 cm. An image of the grid of lesions generated is shown in Figure 7. It can be seen in this image that lesion generation was not appreciably affected as the position of the skullcap/RBC phantom pair with respect to the transducer changed. The lesions generated during this experiment had average radii of 708±71 μm, with minimum and maximum radii of 606 and 879 μm, respectively.

Incidental lesions similar to those observed in Figs. 6(b) & 6(d) may also be seen surrounding the main lesions generated throughout this image. These incidental lesions were observed to have average radii on the order of 100 μm and were observed to be generated on average up to 1.1 mm from the centers of the main lesions, as measured from centroid to centroid of the respective lesions, with a maximum extent of 2.3 mm.

To demonstrate the ability of histotripsy to treat arbitrarily shaped regions through the skullcap without aberration correction and irrespective of the position of the skullcap/RBC phantom pair with respect to the transducer, a lesion in the shape of a 1 cm wide block ‘M’ was also generated by mechanically repositioning the skullcap/RBC phantom pair within the transducer to outline the shape (Fig. 8). The block ‘M’ was generated using histotripsy pulses of the same pressure amplitude as those used to generate the 5 × 5 grid described above, and was generated through skullcap 3. It can be seen that we were effectively able to use histotripsy to create an ‘arbitrary’ pattern through the skullcap without using aberration

correction by mechanically repositioning the skullcap/RBC phantom pair within the transducer.

IV. Discussion

In this paper we have demonstrated the ability of histotripsy to generate targeted cavitation and lesions through excised human skullcaps without using aberration correction. Using 2-cycle pulses at a PRF of 1 Hz, cavitation bubble clouds and lesions were generated through three different skullcaps and with the skullcap/RBC phantom pair at different positions with respect to the transducer. By simple mechanical repositioning, histotripsy can be used to generate arbitrarily shaped lesions through the skullcap without using aberration correction.

Histotripsy's robustness to aberrations introduced by the skullcap has been demonstrated. We have shown that the high-amplitude portions of the pressure waveforms measured at the transducer's focus at the regions within the skullcap targeted during this study are not significantly distorted as they pass through the skullcaps compared to the free field, despite having to increase the driving amplitude of the array to account for losses to attenuation through the skull to acheive equivalent focal pressures amplitudes during transcranial measurements. Reflections of the ultrasound pulses within the skullcaps were observed and seen to have amplitudes significantly lower than the initial high amplitude portion of the pulse responsible for damage. The main lobes of the pressure profiles maintained their shape and size well through the skullcaps, out to about the −5 dB widths, while the side lobes were increased and widened beyond that compared to the free field. While measurements of the pressure amplitudes of the pulses used to generate the lesions shown in this paper could not be made directly due to the limitations cavitation activity puts on hydrophone survival when inserted into the field, estimates of the negative pressure amplitude via linear summation, $(p\text{-})_{LE}$, proved reliable for predicting cavitation activity in the field at the targeted locations. The lesions generated through the skullcaps were generated using histotripsy without using aberration correction. The main lesions were well confined within the main lobe, with minimal incidental lesion generation outside, and their sizes were consistent across the different skullcap samples used. Histotripsy's robustness to aberrations may be attributed to both the short duration pulses ($\leq$2 acoustic cycles) used for treatment and the intrinsic threshold nucleation mechanism by which the cavitation bubble clouds responsible for generating lesions are formed. The first of these two features of histotripsy helps to minimize the side lobes of the pressure field in the focal region and the second ensures that damage is localized to only the region where the pressure exceeds the threshold for cavitation. In effect, despite being increased due to aberrations, the side lobes are effectively 'thresholded out', as cavitation remains confined only to the main lobe where the pressure exceeds the intrinsic threshold.

This robustness to aberrations may be better understood by example, emphasising again that damage produced by histotripsy is highly localized to only the region where the negative pressure exceeds the intrinsic threshold for nucleation, and that the pressure pulses emitted by individual elements of the histotripsy array are ~1.5 acoustic cycles long with only one large peak negative half cycle, similar to what is seen in Figure 4. Importantly, this allows us to neglect the effects of multi-cycle interactions between the negative pressure phases of

subsequent acoustic cycles as they travel through the focal zone, and allows us to make estimations of the expected focal shift based on the intersection points of the large negative half-cycles of the acoustic pulses emitted from each element of the array. If we consider distortions to the focal zone to be primarily the result of phase distortions introduced to the ultrasound pulses as they propogate through the skullcaps, and that constructive interfence between *all* elements of the array are needed to produce negative pressure amplitudes beyond the intrinsic threshold, we can use straight-line ray tracing arguments based on time of flight measurements from individual elements of the histotripsy array to make estimates of the bounding values of the expected shifts in the focal location. Measurements of the relative temporal shifts between pulses from individual elements of the array as they traveled through the skull were measured during experiments to be on the order 1 μs. Based on the geometry of the transducer and the single negative half-cycle nature of the ultrasound pulses used in these studies, and in an idealized case where focal shifts are produced solely by phase distortions between pulses, calculations of the maximum focal expected shift based on these measurements, in tissue with a sound speed on the order of 1.5 mm/μs, are on the order of ≤1.5 mm. Given that each pressure pulse only has one large peak negative half-cycle associated with it, interactions in the field between the negative pressure phases of different acoustic cycles are eliminated as well, severly restricting the range over which adequate constructive interference may exist to produce pressures in excess of the intrinsic threshold, and thereby produce nucleation and damage, as was indeed observed in experiments.

The short duration of the pulses is similarly expected to limit the how the effects of diffraction may distort the focus. While diffraction does occur regardless of pulse length, the pulse length does affect the degree to which diffraction can distort the pressure field owing to the limited number of acoustic cycles associated with each pulse which may interfere with themselves or others in the field. One might consider, for example, an idealized case of an interfence pattern created at some surface in a field generated by two adjacent sources with a fixed separation between them in the 1.5-cycle and CW regimes. In the CW regime, the interference pattern would show a whole series of peaks and minima along the surface of interest corresponding to where path length differences between the waves propogating from each element produced constructive or destructive interference with one another. At 1.5 cycles, however, the pulses would only produce a finite number of minima in the field, corresponding to where the single negative half-cycle destructively interfered with the two surrounding positive half-cycles of the pulse. While the effects of diffraction due to the skull are significantly more complex than those of this example, it serves as a simple illustration of how the outcomes of diffraction can be affected by the pulse length, even though the effect occurs regardless. Because of the short duration nature of the pulses used during these experiments and how they limit the outcomes of diffraction, diffractive effects at the focus are limited and are not expected to significantly distort the main lobe of the pressure field or to produce side lobes in excess of the threshold for cavitation and damage.

Shear mode production of focal points in addition to those generated via longitudinal mode production is another area of interest and concern associated with transcranial therapies [45]–[47]. Particularly, owing to the sound speed differences between shear and longitudinal waves in bone (1400 m/s vs. 2330 m/s @ 0.3–0.8 MHz) [15], [44], [46], phase aberrations and refractive effects can lead to the production of two separate focal points in the field

associated with each mode of transmission. However, because the shear wave speed in bone is more closely matched to that of water/brain than the longitudinal modes, distortions of the shear waves due to refraction are expected to be less severe than those experienced by longitudinal waves, as are temporal distortions in their arrival times owing to the similarity in sound speeds between the media. Because the individual distortions experienced by shear waves are less severe than those experienced by longitudinal waves, the focal point generated by shear waves is likely to be less distorted overall than that produced by longitudinal waves. However, because of the comparatively high attenuation of shear waves compared to longitudinal waves in the skull bone [23], [46], [47], the pressure amplitudes at potential focal points generated by shear waves are not expected to be high enough to produce cavitation or damage, and may be thresholded out during procedures by limiting the driving amplitude of the therapy array to ensure the pressure threshold is not exceeded at the shear mode focus.

Non-linear effects owing to the high pressures of the pulses emenating from individual elements of the array are also expected to minimally affect the focus. While the pressure amplitudes of the pulses in the free field are sufficient to generate nonlinear effects, the skullcaps act to efficiently attenuate the high amplitude pulses and filter out their high frequency content as they pass through the skull [15], [44], [48]. Owing to the reduced amplitude of the pulses after passing through the skullcaps and the reduced propagation distance from the skullcap surface to the focus, the subsequent development of non-linearities en route to the focus is expected to minimally affect the focus. Owing to the short duration of the pulses, thermal effects from pulses that do exhibit nonlinearities are expected to be negligible. In addition, it has been shown that the effects of non-linearities only minimally effect the phasing of pulses as they propagate to the focus through the skull [48] and so should not be expected to contribute significantly to focal distortions owing to phase aberrations induced by the non-linearities between pulses.

Lesions generated in the RBC phantoms demonstrate that histotripsy can be applied transcranially without using aberration correction through a variety of different skullcaps with minimal extraneous damage. The location of cavitation events and lesion generation were observed to be predictable and repeatable throughout these experiments at the geometric origin of the transducer. This may be attributed to the intrinsic threshold nucleation mechanism used to generate the cavitation bubble clouds and the small volume in the focal region over which pressures exceed the intrinsic threshold as described above, as well as the low PRF at which the pulses were applied (1 Hz) during treatment compared to other studies ($\geq$ 100 Hz) [26]. Further improvements in precision during these treatments may additionally be gained by reducing the pressure amplitudes of the pulses used to generate lesions to just above the threshold for nucleation to reduce the incidence of extraneous lesion formation as was observed at the higher amplitudes used to generate the lesions in Figs. 7 & 8. While applying histotripsy through the skullcap without aberration correction may not be suited for all applications, particularly those requiring precision greater than can be offered without it, it does open the door for creating a much simplified and potentially lower cost treatment option compared to those involving sophisticated aberration correction using CT and MRI [19], [20], as it removes the necessity of additional manpower and machine time in order to carry out.

We have also shown that lesions can be generated at the transducer's focus through the skullcap with the skullcap/RBC phantom pair at different locations with respect to the transducer without using aberration correction. The size and shape of the lesions generated in this way were consistent across the different positions at which they were produced and the position of the skullcap/RBC phantom pair with respect to the transducer did not appreciably affect their generation. The positions of the lesions relative to the fixed grid points onto which they were mechanically steered was similarly minimally affected by the position of the skullcap/RBC phantom pair with respect to the transducer, i.e., the position of the skullcap within the transducer did not introduce significant spatial aberrations to the location of the transducer's focal point, with a maximum observed offset between the steering location and lesion center of less than 300 μm, in good agreement with measurements of the spatial profiles of the pressure fields. While this study only looked at focal shifts in the transverse direction of the transducer, it demonstrates that aberrations introduced by the skullcap as its position with respect to the transducer is changed do not significantly affect the transverse location of the histotripsy focal point and do not axially shift the extent of the bubble cloud out of the plane of the RBC layer of the phantom.

We have also demonstrated the ability of histotripsy to form arbitrarily shaped lesions through the skullcap without aberration correction by mechanically repositioning the skullcap/RBC phantom pair with respect to the transducer to generate a lesion in the shape of a block 'M'. This type of treatment demonstrates that by incrementally moving the subject or the transducer, histotripsy may be used to generate arbitrarily shaped contiguous lesions through the skullcap. This type of treatment option is important for applications where the treatment volume might be larger than the histotripsy focal volume, for instance in cases of intracerebral hemorrhage and brain tumor.

Histotripsy provides further advantages over other ultrasound based therapies in the form of reduced heating to the skullcap as the ultrasound pulses pass through it, despite the high amplitude pulses used for treatment and the high ultrasound absorption of bone. This is due to the short duration (≤2 acoustic cycles) and inherently lower duty cycle of the pulses used to generate the cavitation bubble clouds responsible for lesion generation during histotripsy compared to other cavitation or thermal based ultrasound therapies (≥100 acoustic cycles). While standard strategies of reducing skullcap heating during ultrasound therapies would not be precluded from use with histotripsy should the need arise, this has the potential to allow for faster treatment times as higher pulse repetition frequencies may be used during treatment before incurring significant thermal heating problems associated with ultrasound absorption by the skull bone. This also has the potential to mitigate the need to actively cool the skullcap during therapy to prevent thermal damage to the skull bone [21], [25], and thereby simplify the protocol for delivering this type of ultrasound therapy.

V. Conclusion

The feasibility of applying histotripsy transcranially without using aberration correction has been demonstrated. Because of the very sharp threshold phenomenon, side-lobes below the intrinsic threshold have very little effect on the shape of the generated bubble cloud and, therefore, on the shape of the produced lesion. We have shown that histotripsy can be used to

generate targeted lesions through a variety of different skullcaps with different characteristic dimensions and attenuations. Lesion generation was achieved with the skullcap/RBC phantom pair at different positions with respect to the transducer. We have also demonstrated that histotripsy may be used to generate arbitrarily shaped lesions through the skullcap by incrementally repositioning the skullcap/RBC phantom pair with respect to the transducer during treatment to target different regions.

Acknowledgements

The authors thank D. A. Mueller and the Anatomical Donations Program at the University of Michigan for providing the skull samples used in this study. This work is supported by grants from the National Institute of Biomedical Imaging and Bioengineering (NIBIB) of the National Institutes of Health under Award Number R01EB008998, NIH grant R01 CA134579, and National Science Foundation (S10 RR022425) Disclosure: Drs. Charles A. Cain, Zhen Xu, and Timothy L. Hall have financial interest and/or other relationship with HistoSonics Inc.

Biography

Jonathan R. Sukovich is a postdoctoral fellow in the Department of Biomedical Engineering at the University of Michigan. He received a B.S. and Ph.D. degrees in mechanical engineering from Boston University in 2008 and 2013, respectively where he studied laser interactions with water at high pressures and phenomena associated with high energy bubble collapse events. He joined the University of Michigan in the summer of 2013 to study histotripsy for brain applications. His research interests include high energy bubble collapse phenomena, focused ultrasound therapies, and acoustic cavitation.

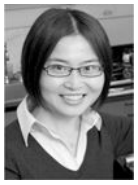

Zhen Xu (S’05-M’06’) is an Associate Professor in the Department of Biomedical Engineering at the University of Michigan, Ann Arbor, MI. She received the B.S.E. (highest honors) degree in biomedical engineering from Southeast University, Nanjing, China, in 2001, and her M.S. and Ph.D. degrees from the University of Michigan in 2003 and 2005, respectively, both in biomedical engineering. Her research is focusing on ultrasound therapy, particularly the applications of histotripsy for noninvasive surgeries. In 2006, she received IEEE Ultrasonics, Ferroelectrics and Frequency Control Society Outstanding Paper Award; American Heart Association (AHA) Outstanding research in Pediatric Cardiology in 2010; National Institute of Health (NIH) New Investigator Award at the First National Institute of Biomedical Imaging and Bioengineering (NIBIB) Edward C. Nagy New Investigator Symposium in 2011, and Frederic Lizzi Early Career Award from the International Society

of Therapeutic Ultrasound (ISTU) in 2015. She is an associated editor for IEEE Transactions on Ultrasonics, Ferroelectrics, and Frequency Control (UFFC).

Yohan Kim received his B.S. degree in electrical engineering from the University of Texas at Austin in 2006, his M.S. degree in electrical engineering and Ph.D. in biomedical engineering, both from the University of Michigan, Ann Arbor, in 2009 and 2013, respectively. After completing his postdoctoral fellowship in 2014, Yohan joined Medtronic plc where he is investigating novel therapeutic modalities for neuromodulation applications. His research interests include non-invasive therapeutic ultrasound, phased array transducer development and RF electronics for biomedical applications.

Hui Cao was born in 1969 in Xi'an, Shaanxi China. He received his Ph.D. in 2004 from Shaanxi Normal University where he is currently an associate professor in the applied acoustics laboratoy and his research is primarily focused on the development of ultrasonic motors. Dr. Cao was a visiting scholar at the University of Michigan from 2013 to 2014 where he helped design and build ultrasonic arrays and the electronics for driving them.

Thai-Son Nguyen is an undergraduate student at the University of Michigan majoring in Biomedical Engineering and is expected to receive his B.S.E. in 2015. He joined the Image-Guided Ultrasound Therapy Laboratory in 2013 as a research assistant assisting with histotripsy experiments for brain applications.

Aditya S. Pandey, M.D. achieved his Bachelors of Science in Biological and Engineering Sciences from the Washington University in St. Louis. He obtained his Doctorate of Medicine from Case Western Reserve University School of Medicine. He then gained

training in neurological surgery with sub-specialty training in microsurgical and endovascular treatment of cerebrovascular disorders. Dr. Pandey specializes in treating individuals who have blood vessel related diseases of the brain and spinal cord (e.g., aneurysms, AVM, stroke, fistulas, cavernomas, etc.) as well as practicing general neurosurgery (spinal disorders, brain tumors, and traumatic brain injury).

He is one of two neurosurgeons in the Ann Arbor region who are trained to perform both open surgeries and endovascular radiological procedures when treating brain blood vessel related diseases. His research interests are aimed at developing and improving tools to assist in the fight against stroke and brain aneurysms. He has been the author of more than 30 research publications as well as participated in numerous national research trials aimed at improving techniques of aneurysm treatment. Dr. Pandey is currently leading a study to better understand whether a patient requiring aneurysm treatment should be maintained on seizure medications post surgery.

Timothy L. Hall was born in 1975 in Lansing, MI. He is currently an assistant research scientist in the Department of Biomedical Engineering at the University of Michigan. He received the B.S.E. degree in 1998 and the M.S.E. degree in 2001, both in electrical engineering, and he received his Ph.D. degree in 2007 in biomedical engineering, all from the University of Michigan. He worked for Teradyne Inc., Boston, MA, from 1998 to 1999 as a circuit design engineer and at the University of Michigan from 2001 to 2004 as a visiting research investigator. His research interests are in high-power pulsed-RF-amplifier electronics, phased-array ultrasound transducers for therapeutics, and sonic cavitation for therapeutic applications.

Charles A. Cain (S’65M’71SM’80F’89) was born in Tampa, FL, on March 3, 1943. He received the B.E.E. (highest honors) degree in 1965 from the University of Florida, Gainesville, FL; the M.S.E.E. degree in 1966 from the Massachusetts Institute of Technology, Cambridge, MA; and the Ph.D. degree in electrical engineering in 1972 from the University of Michigan, Ann Arbor, MI. From 1965 through 1968, he was a member of the Technical Staff at Bell Laboratories, Naperville, IL, where he worked in the electronic switching systems development area. From 1972 through 1989, he was in the Department of Electrical and Computer Engineering at the University of Illinois at UrbanaChampaign, where he was a professor of electrical engineering and bioengineering. Since 1989, he has

been in the College of Engineering at the University of Michigan, Ann Arbor, as a professor of biomedical engineering and electrical engineering. He was the chair of the Biomedical Engineering Program from 1989 to 1996, the founding chair of the Biomedical Engineering Department from 1996 to 1999, and the Richard A. Auhll Professor of Engineering in 2002. He has been involved in research on the medical applications of ultrasound, particularly high-intensity ultrasound for noninvasive surgery. He was formerly an associate editor of the IEEE Transactions on Biomedical Engineering and the IEEE Transactions on Ultrasonics, Ferroelectrics, and Frequency Control, and an editorial board member of the International Journal of Hyperthermia and Radiation Research. He is a fellow of IEEE and the American Institute for Medical and Biological Engineering (AIMBE).

References

[1]. Lynn JG and Putnam TJ, "Histology of cerebral lesions produced by focused ultrasound," The American journal of pathology, vol. 20, no. 3, p. 637, 1944. [PubMed: 19970769]

[2]. Fry WJ, Mosberg W Jr, Barnard J, and Fry F, "Production of focal destructive lesions in the central nervous system with ultrasound*," Journal of neurosurgery, vol. 11, no. 5, pp. 471–478, 1954. [PubMed: 13201985]

[3]. Barnard J, Fry W, Fry F, and Brennan J, "Small localized ultrasonic lesions in the white and gray matter of the cat brain," AMA Archives of Neurology & Psychiatry, vol. 75, no. 1, pp. 15–35, 1956. [PubMed: 13275157]

[4]. Young G and Lele P, "Focal lesions in the brain of growing rabbits produced by focused ultrasound," Experimental Neurology, vol. 9, no. 6, pp. 502–511, 1964. [PubMed: 14188536]

[5]. Fry F, "Transkull transmission of an intense focused ultrasonic beam," Ultrasound in medicine & biology, vol. 3, no. 2, pp. 179–184, 1977. [PubMed: 595211]

[6]. Tempany CM, McDannold NJ, Hynynen K, and Jolesz FA, "Focused ultrasound surgery in oncology: overview and principles," Radiology, vol. 259, no. 1, pp. 39–56, 2011. [PubMed: 21436096]

[7]. Jeanmonod D, Werner B, Morel A, Michels L, Zadicario E, Schiff G, and Martin E, "Transcranial magnetic resonance imaging–guided focused ultrasound: noninvasive central lateral thalamotomy for chronic neuropathic pain," Neurosurgical focus, vol. 32, no. 1, p. E1, 2012.

[8]. Elias WJ, Huss D, Voss T, Loomba J, Khaled M, Zadicario E, Frysinger RC, Sperling SA, Wylie S, Monteith SJ, et al., "A pilot study of focused ultrasound thalamotomy for essential tremor," New England Journal of Medicine, vol. 369, no. 7, pp. 640–648, 2013. [PubMed: 23944301]

[9]. Meairs S, Alonso A, and Hennerici MG, "Progress in sonothrombolysis for the treatment of stroke," Stroke, vol. 43, pp. 1706–1710, 6 2012. [PubMed: 22535275]

[10]. Alexandrov AV, "Ultrasound enhancement of fibrinolysis," Stroke; A Journal of Cerebral Circulation, vol. 40, pp. S107–S110, 3 2009.

[11]. Monteith SJ, Harnof S, Medel R, Popp B, Wintermark M, Lopes MBS, Kassell NF, Elias WJ, Snell J, Eames M, et al., "Minimally invasive treatment of intracerebral hemorrhage with magnetic resonance–guided focused ultrasound: laboratory investigation," Journal of neurosurgery, vol. 118, no. 5, pp. 1035–1045, 2013. [PubMed: 23330996]

[12]. Hynynen K, McDannold N, Vykhodtseva N, Raymond S, Weissleder R, Jolesz FA, and Sheikov N, "Focal disruption of the blood-brain barrier due to 260-khz ultrasound bursts: a method for molecular imaging and targeted drug delivery," Journal of neurosurgery, vol. 105, no. 3, pp. 445–454, 2006. [PubMed: 16961141]

[13]. Choi JJ, Selert K, Gao Z, Samiotaki G, Baseri B, and Konofagou EE, "Noninvasive and localized blood–brain barrier disruption using focused ultrasound can be achieved at short pulse lengths and low pulse repetition frequencies," Journal of Cerebral Blood Flow & Metabolism, vol. 31, no. 2, pp. 725–737, 2010. [PubMed: 20842160]

[14]. Coluccia D, Fandino J, Schwyzer L, OGorman R, Remonda L, Anon J, Martin E, and Werner B, "First noninvasive thermal ablation of a brain tumor with mr-guided focused ultrasound," Journal of Therapeutic Ultrasound, vol. 2, no. 1, p. 17, 2014. [PubMed: 25671132]

[15]. Fry F and Barger J, "Acoustical properties of the human skull," The Journal of the Acoustical Society of America, vol. 63, no. 5, pp. 1576–1590, 1978. [PubMed: 690336]

[16]. Hynynen K and Jolesz FA, "Demonstration of potential noninvasive ultrasound brain therapy through an intact skull," Ultrasound in medicine & biology, vol. 24, no. 2, pp. 275–283, 1998. [PubMed: 9550186]

[17]. Pernot M, Aubry J-F, Tanter M, Thomas J-L, and Fink M, "High power transcranial beam steering for ultrasonic brain therapy," Physics in medicine and biology, vol. 48, no. 16, p. 2577, 2003. [PubMed: 12974575]

[18]. Gâteau J, Marsac L, Pernot M, Aubry J-F, Tanter M, and Fink M, "Transcranial ultrasonic therapy based on time reversal of acoustically induced cavitation bubble signature," Biomedical Engineering, IEEE Transactions on, vol. 57, no. 1, pp. 134–144, 2010.

[19]. Marquet F, Pernot M, Aubry J, Montaldo G, Marsac L, Tanter M, and Fink M, "Non-invasive transcranial ultrasound therapy based on a 3d ct scan: protocol validation and in vitro results," Physics in medicine and biology, vol. 54, no. 9, p. 2597, 2009. [PubMed: 19351986]

[20]. McDannold N, Clement G, Black P, Jolesz F, and Hynynen K, "Transcranial mri-guided focused ultrasound surgery of brain tumors: Initial findings in three patients," Neurosurgery, vol. 66, no. 2, p. 323, 2010. [PubMed: 20087132]

[21]. Pernot M, Aubry J-F, Tanter M, Boch A-L, Marquet F, Kujas M, Seilhean D, and Fink M, "In vivo transcranial brain surgery with an ultrasonic time reversal mirror," Journal of neurosurgery, vol. 106, no. 6, pp. 1061–1066, 2007. [PubMed: 17564179]

[22]. Pinton G, Aubry J-F, Bossy E, Muller M, Pernot M, and Tanter M, "Attenuation, scattering, and absorption of ultrasound in the skull bone," Medical physics, vol. 39, no. 1, pp. 299–307, 2012. [PubMed: 22225300]

[23]. White P, Clement G, and Hynynen K, "Longitudinal and shear mode ultrasound propagation in human skull bone," Ultrasound in medicine & biology, vol. 32, no. 7, pp. 1085–1096, 2006. [PubMed: 16829322]

[24]. McDannold N, King RL, and Hynynen K, "MRI monitoring of heating produced by ultrasound absorption in the skull: in vivo study in pigs," Magnetic resonance in medicine, vol. 51, no. 5, pp. 1061–1065, 2004. [PubMed: 15122691]

[25]. Connor CW and Hynynen K, "Patterns of thermal deposition in the skull during transcranial focused ultrasound surgery," Biomedical Engineering, IEEE Transactions on, vol. 51, no. 10, pp. 1693–1706, 2004.

[26]. Gateau J, Aubry J, Chauvet D, Boch A, Fink M, and Tanter M, "In vivo bubble nucleation probability in sheep brain tissue," Physics in medicine and biology, vol. 56, no. 22, p. 7001, 2011. [PubMed: 22015981]

[27]. Monteith SJ, Kassell NF, Goren O, and Harnof S, "Transcranial mr-guided focused ultrasound sonothrombolysis in the treatment of intracerebral hemorrhage," Neurosurgical focus, vol. 34, no. 5, p. E14, 2013. [PubMed: 23634918]

[28]. Hynynen K, McDannold N, Sheikov NA, Jolesz FA, and Vykhodtseva N, "Local and reversible blood–brain barrier disruption by noninvasive focused ultrasound at frequencies suitable for trans-skull sonications," Neuroimage, vol. 24, no. 1, pp. 12–20, 2005. [PubMed: 15588592]

[29]. McDannold N, Vykhodtseva N, and Hynynen K, "Targeted disruption of the blood–brain barrier with focused ultrasound: association with cavitation activity," Physics in medicine and biology, vol. 51, no. 4, p. 793, 2006. [PubMed: 16467579]

[30]. Kinoshita M, McDannold N, Jolesz FA, and Hynynen K, "Noninvasive localized delivery of herceptin to the mouse brain by mri-guided focused ultrasound-induced blood–brain barrier disruption," Proceedings of the National Academy of Sciences, vol. 103, no. 31, pp. 11719–11723, 2006.

[31]. Kinoshita M, McDannold N, Jolesz FA, and Hynynen K, "Targeted delivery of antibodies through the blood–brain barrier by mri-guided focused ultrasound," Biochemical and biophysical research communications, vol. 340, no. 4, pp. 1085–1090, 2006. [PubMed: 16403441]

[32]. Holland CK, Vaidya SS, Datta S, Coussios C-C, and Shaw GJ, "Ultrasound-enhanced tissue plasminogen activator thrombolysis in an *in vitro* porcine clot model," Thrombosis research, vol. 121, no. 5, pp. 663–673, 2008. [PubMed: 17854867]

[33]. Datta S, Coussios C-C, McAdory LE, Tan J, Porter T, De Courten-Myers G, and Holland CK, "Correlation of cavitation with ultrasound enhancement of thrombolysis," Ultrasound in medicine & biology, vol. 32, no. 8, pp. 1257–1267, 2006. [PubMed: 16875959]

[34]. Datta S, Coussios C-C, Ammi AY, Mast TD, de Courten-Myers GM, and Holland CK, "Ultrasound-enhanced thrombolysis using definity R as a cavitation nucleation agent," Ultrasound in medicine & biology, vol. 34, no. 9, pp. 1421–1433, 2008. [PubMed: 18378380]

[35]. Hitchcock KE and Holland CK, "Ultrasound-assisted thrombolysis for stroke therapy better thrombus break-up with bubbles," Stroke, vol. 41, no. 10 suppl 1, pp. S50–S53, 2010. [PubMed: 20876505]

[36]. Maxwell AD, Cain CA, Hall TL, Fowlkes JB, and Xu Z, "Probability of cavitation for single ultrasound pulses applied to tissues and tissue-mimicking materials," Ultrasound in medicine & biology, vol. 39, no. 3, pp. 449–465, 2013. [PubMed: 23380152]

[37]. Kim Y, Wang T-Y, Xu Z, and Cain CA, "Lesion generation through ribs using histotripsy therapy without aberration correction," Ultrasonics, Ferroelectrics and Frequency Control, IEEE Transactions on, vol. 58, no. 11, pp. 2334–2343, 2011.

[38]. Lin K-W, Duryea A, Kim Y, Hall T, Xu Z, and Cain C, "Dual-beam histotripsy: a low-frequency pump enabling a high-frequency probe for precise lesion formation," Ultrasonics, Ferroelectrics, and Frequency Control, IEEE Transactions on, vol. 61, no. 2, pp. 325–340, 2014.

[39]. Lin K-W, Kim Y, Maxwell AD, Wang T-Y, Hall TL, Xu Z, Fowlkes JB, and Cain C, "Histotripsy beyond the intrinsic cavitation threshold using very short ultrasound pulses: microtripsy," Ultrasonics, Ferroelectrics, and Frequency Control, IEEE Transactions on, vol. 61, no. 2, pp. 251–265, 2014.

[40]. Kim Y, Hall T, Xu Z, and Cain C, "Transcranial histotripsy therapy: a feasibility study," Ultrasonics, Ferroelectrics and Frequency Control, IEEE Transactions on, vol. 61, no. 4, pp. 582–593, 2014.

[41]. Kim Y, Maxwell AD, Hall TL, Xu Z, Lin K-W, and Cain CA, "Rapid prototyping fabrication of focused ultrasound transducers," Ultrasonics, Ferroelectrics, and Frequency Control, IEEE Transactions on, vol. 61, no. 9, pp. 1559–1574, 2014.

[42]. Parsons JE, Cain CA, and Fowlkes JB, "Cost-effective assembly of a basic fiber-optic hydrophone for measurement of high-amplitude therapeutic ultrasound fields," The Journal of the Acoustical Society of America, vol. 119, p. 1432, 2006. [PubMed: 16583887]

[43]. Maxwell AD, Wang T-Y, Yuan L, Duryea AP, Xu Z, and Cain CA, "A tissue phantom for visualization and measurement of ultrasound-induced cavitation damage," Ultrasound in medicine & biology, vol. 36, no. 12, pp. 2132–2143, 2010. [PubMed: 21030142]

[44]. Pichardo S, Sin VW, and Hynynen K, "Multi-frequency characterization of the speed of sound and attenuation coefficient for longitudinal transmission of freshly excised human skulls," Physics in medicine and biology, vol. 56, no. 1, p. 219, 2011. [PubMed: 21149950]

[45]. Cassereau D and Guyomar D, "Computation of the impulse diffraction of any obstacle by impulse ray modelingprediction of the signal distortions," The Journal of the Acoustical Society of America, vol. 84, no. 4, pp. 1504–1516, 1988.

[46]. Clement G, White P, and Hynynen K, "Enhanced ultrasound transmission through the human skull using shear mode conversion," The Journal of the Acoustical Society of America, vol. 115, no. 3, pp. 1356–1364, 2004. [PubMed: 15058357]

[47]. Pichardo S and Hynynen K, "Treatment of near-skull brain tissue with a focused device using shear-mode conversion: a numerical study," Physics in medicine and biology, vol. 52, no. 24, p. 7313, 2007. [PubMed: 18065841]

[48]. Pinton G, Aubry J-F, Fink M, and Tanter M, "Effects of nonlinear ultrasound propagation on high intensity brain therapy," Medical physics, vol. 38, no. 3, pp. 1207–1216, 2011. [PubMed: 21520833]

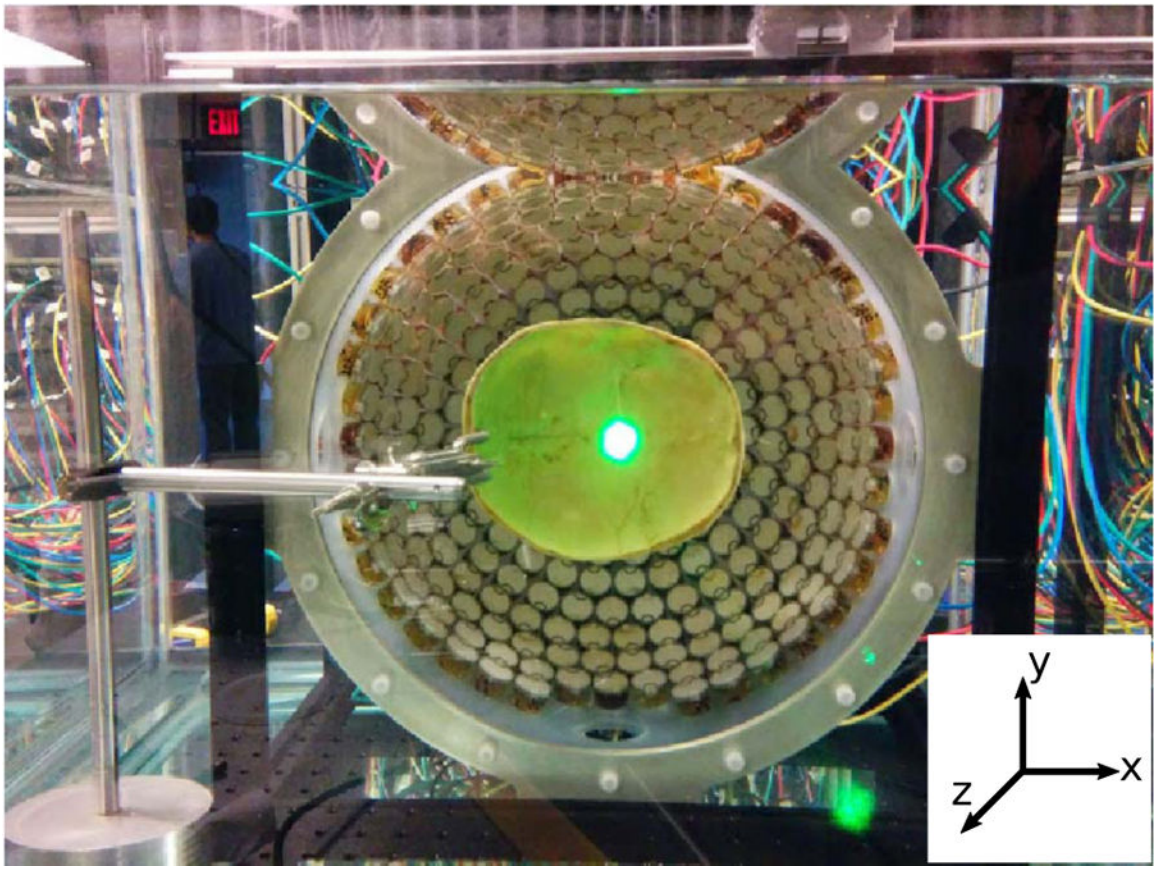

Fig. 1.

An image of the 500 kHz 256-element transducer used to deliver histotripsy treatments with a skullcap mounted within it. The bright spot seen in the center of the skullcap is the reflected laser light used for backlighting the images of the bubble clouds and lesions generated in the RBC phantoms (not shown).

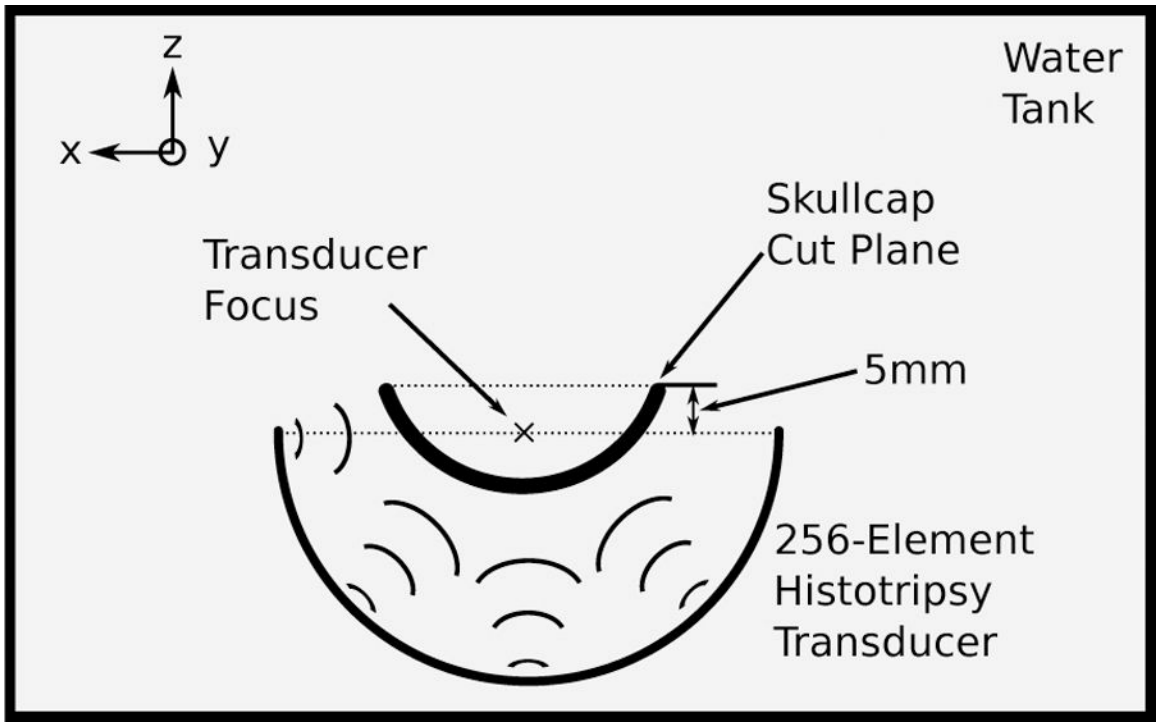

Fig. 2.
Schematic drawing showing the alignment of the transducer's focus within the skullcap.

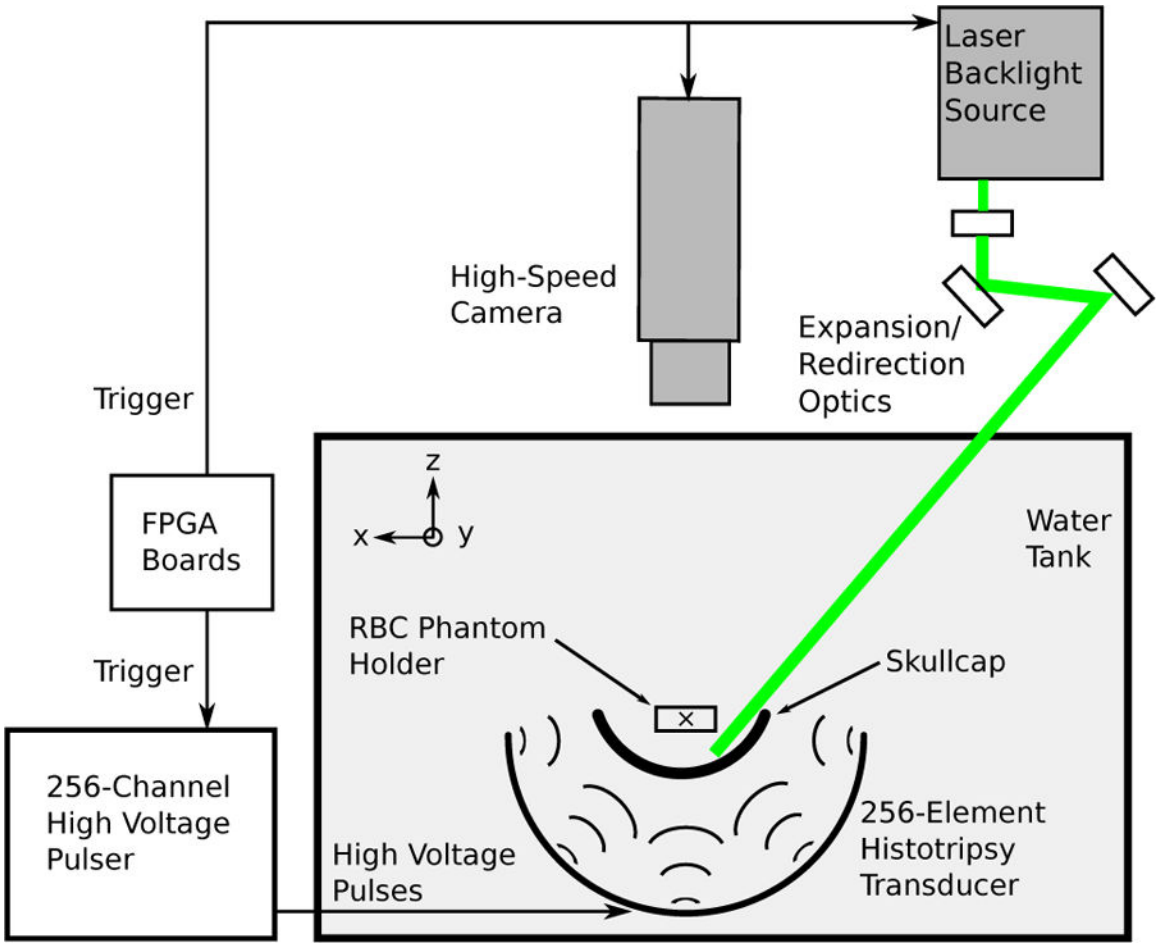

Fig. 3.

Schematic of the experimental setup used for imaging experiments studying single lesion generation through the skullcap. A computer was used to send a trigger signal to the camera and laser for imaging purposes and to the FPGA boards to fire the high voltage pulser responsible for generating the ultrasound pulses used for treatment.

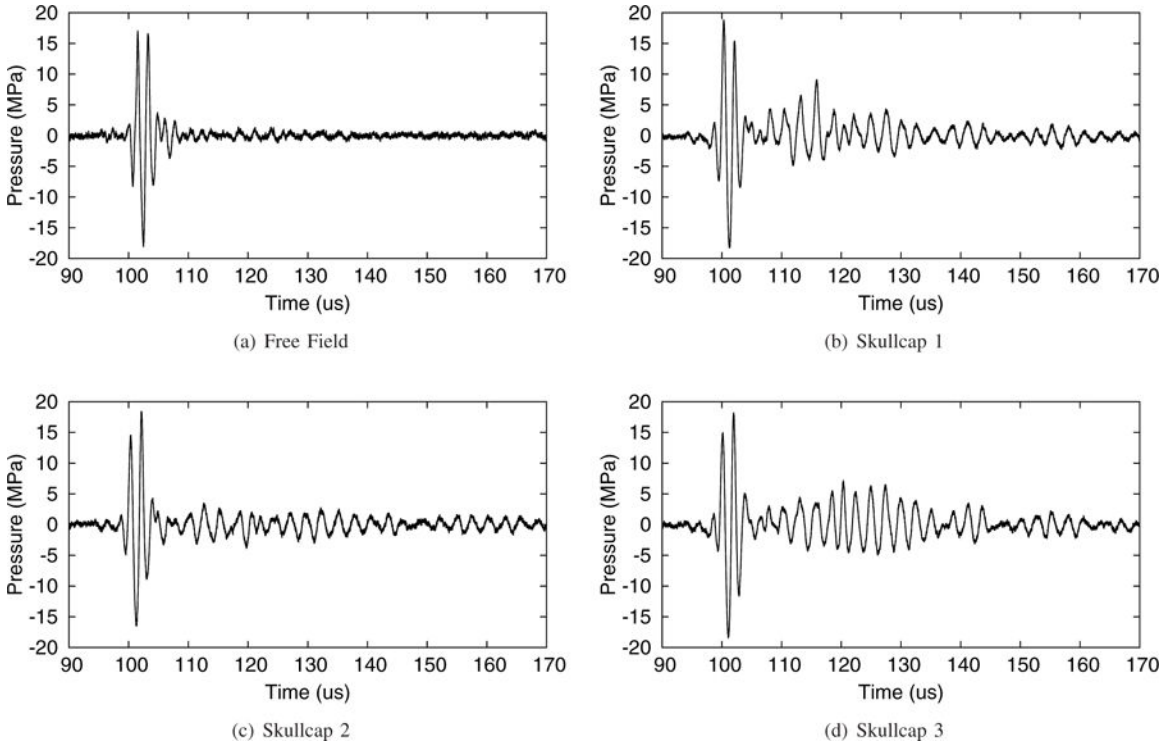

Fig. 4.

Direct measurements of the pressure waveforms at the transducer focus in the free field and through the three skullcaps using a fiber optic hydrophone.

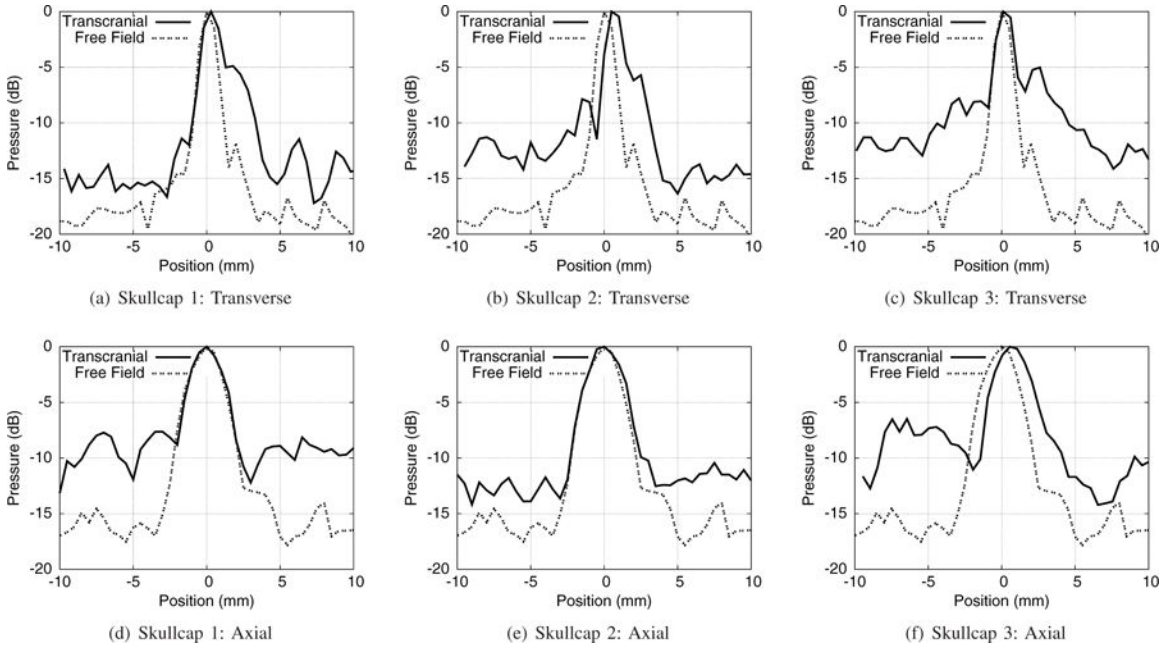

Fig. 5.

Comparison plots of the pressure profiles measured through the skullcaps in comparison to the free field in the transverse (**x**) and axial (**z**) directions of the transducer.

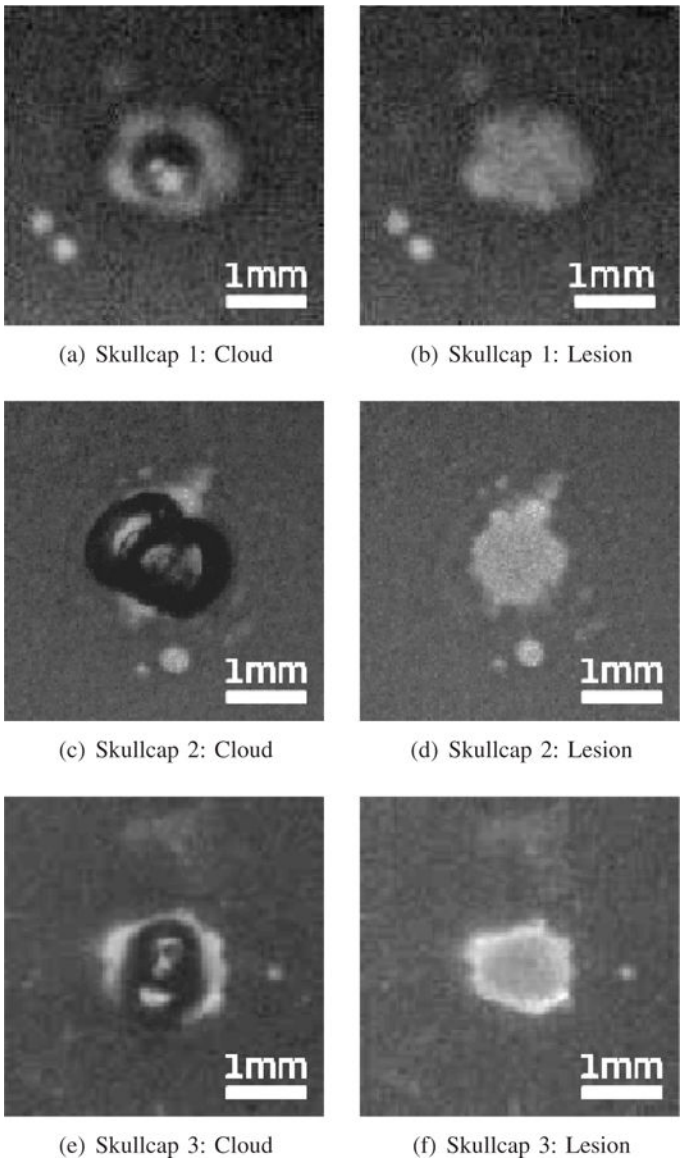

(a) Skullcap 1: Cloud (b) Skullcap 1: Lesion

(c) Skullcap 2: Cloud (d) Skullcap 2: Lesion

(e) Skullcap 3: Cloud (f) Skullcap 3: Lesion

Fig. 6.

Typical bubble clouds and lesions generated in RBC phantoms without aberration correction through the skullcaps used in experiments. The left column shows typical cavitation bubbles generated during treatment (the dark central regions) and the right column shows typical lesions (the bright central regions)

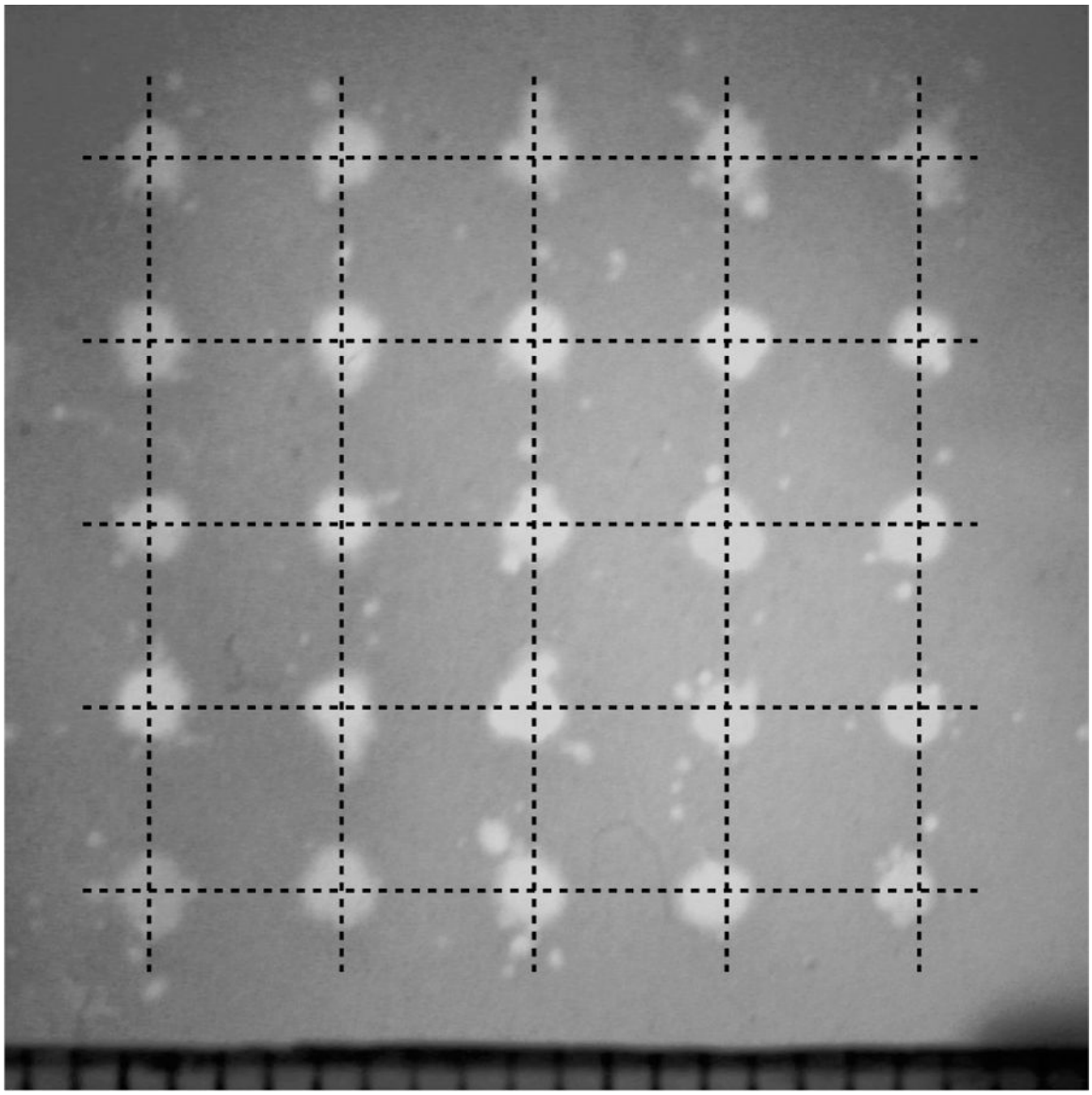

Fig. 7.

An image showing the grid of lesions generated through Skullcap 3 by mechanically repositioning the skullcap with respect to the transducer in 4 mm increments to generate a 1.6×1.6 cm square grid. The intesection points of the grid lines overlaying this image represent the fixed points onto which lesion generation was mechanically steered. These lesions were generated by applying histotripsy pulses through the skullcap without using aberration correction.

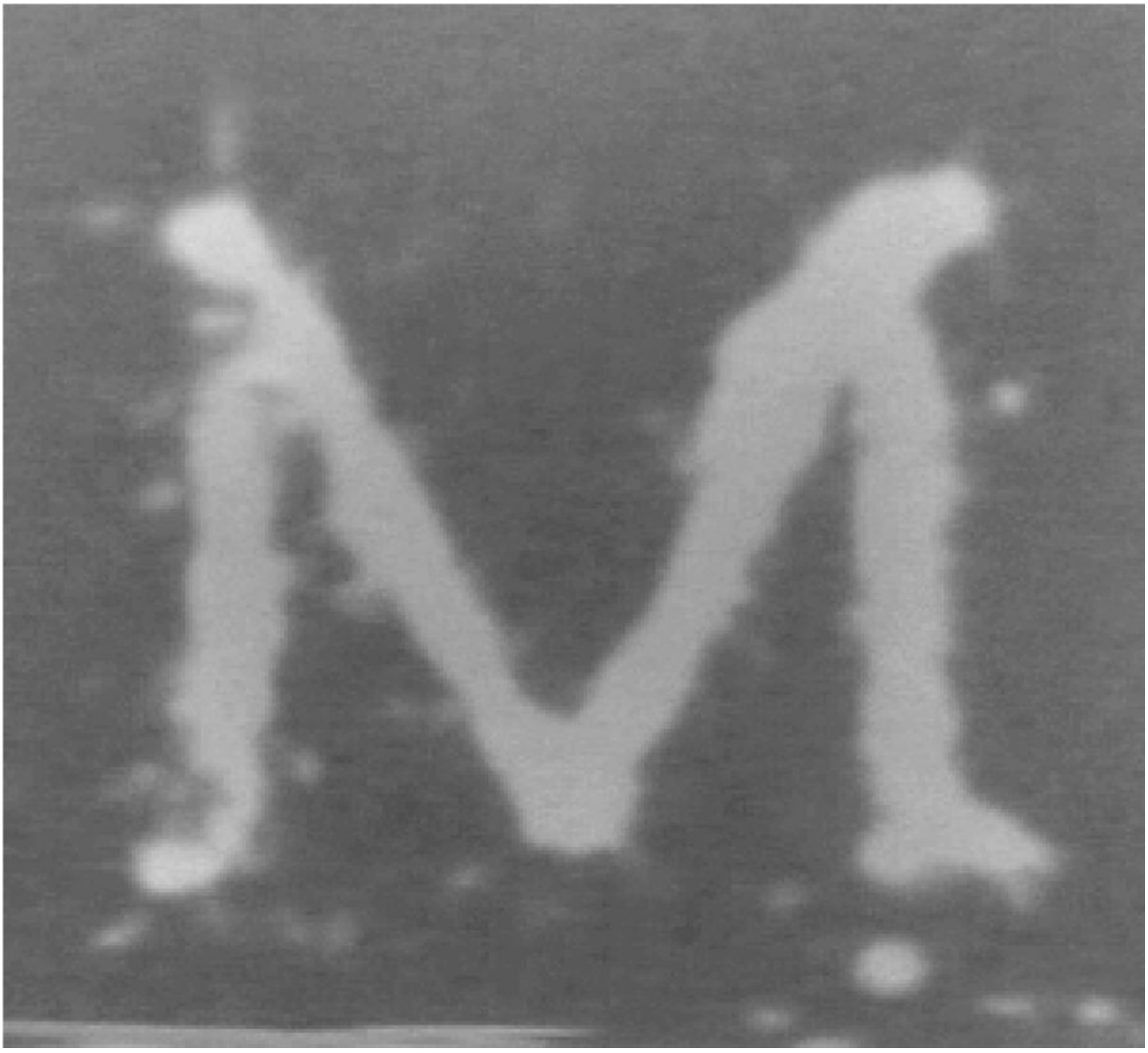

Fig. 8.

An image showing a patterned lesion in the shape of a 1 cm wide block ‘M’ generated through Skullcap 3 by mechanically repositioning the skullcap with respect to the transducer to generate the lesion. This lesion was generated by applying histotripsy pulses through the skullcap without using aberration correction.

TABLE I

MEASUREMENTS OF THE SKULL CAPS USED DURING EXPERIMENTS

Skull Number	Major Dimensions (cm)[1]			Thickness (mm)[2]		Measured Attenuation[3]
	Long Axis	Short Axis	Depth	Min	Max	
1	16.1	13.9	5	2.5	7	78%
2	17.3	14.5	5	5	12	81%
3	18.3	14.3	6	2	12	73%

[1]The long and short axes measurements correspond to the maximum front-to-back and side-to-side dimensions of the skullcap, respectively, measured along the exterior surface of the cut plane of the skullcap. The depth measurements corresponds to the maximum distance from the interior surface of the skull to the cut plane of the skull.

[2]Thickness measurements were made along the cut plane of the skullcap.

[3]The attenuation was measured via fiber optic hydrophone as the reduction in the peak negative pressure amplitude of the array through the skullcap compared to the free field at the geometric focus of the transducer at a fixed driving power such that the free field negative pressure amplitude was measured to be 18 MPa.

IEEE Trans Ultrason Ferroelectr Freq Control. Author manuscript; available in PMC 2020 July 20.

TABLE II

−3 dB WIDTHS OF THE PRESSURE PROFILES MEASURED THROUGH THE THREE SKULLCAP SAMPLES

Sample	Transverse Directions		Axial Direction
	x (mm)	y (mm)	z (mm)
Free Field	1.09	1.12	2.35
Skull 1	1.67	1.35	2.41
Skull 2	1.98	1.2	2.65
Skull 3	1.96	1.26	2.64

TABLE III

RADII OF THE BUBBLE CLOUDS AND LESIONS GENERATED THROUGH THE THREE SKULLCAP SAMPLES

Skull #	N Samples	Bubble Cloud Radii (μm)	Lesion Radii (μm)
1	10	739 ± 148	637 ± 66
2	7	765 ± 243	657 ± 59
3	11	728 ± 118	602 ± 72